

CASE REPORT

Solid Variant Aneurysmal Bone Cyst in Ischiopubic Ramus: A Case Report

KH Chu¹, WK Kung¹, L Xu¹, TWY Chin¹, LK Tse², JW Liao², MK Chan¹

¹Department of Diagnostic and Interventional Radiology, Queen Elizabeth Hospital, Hong Kong SAR, China

²Department of Pathology, Queen Elizabeth Hospital, Hong Kong SAR, China

CASE PRESENTATION

A 39-year-old male presented in December 2022 with a fever of unknown origin. Positron emission tomography–computed tomography (PET-CT) was performed to search for a potential source of sepsis. The patient did not report any symptoms of pain or swelling throughout the evaluation. Nonetheless, an incidental finding of a bone lesion in the left ischiopubic ramus prompted further investigation and an orthopaedic referral.

The lesion appeared subtle and poorly defined on the pelvic radiograph. PET-CT revealed a lytic intramedullary lesion in the left ischiopubic ramus, with no periosteal reaction or soft tissue mass (Figure 1). No pathological fracture was observed. The lesion was hypermetabolic with a maximum standard uptake value of 13.5. Magnetic resonance imaging (MRI) revealed predominantly T1-weighted hypointense signals and T2-weighted hyperintense signals with contrast enhancement (Figure 2). Perilesional bone marrow oedema was noted, along with cortical disruption and adjacent soft tissue oedema at the medial aspect of the left ischial bone.

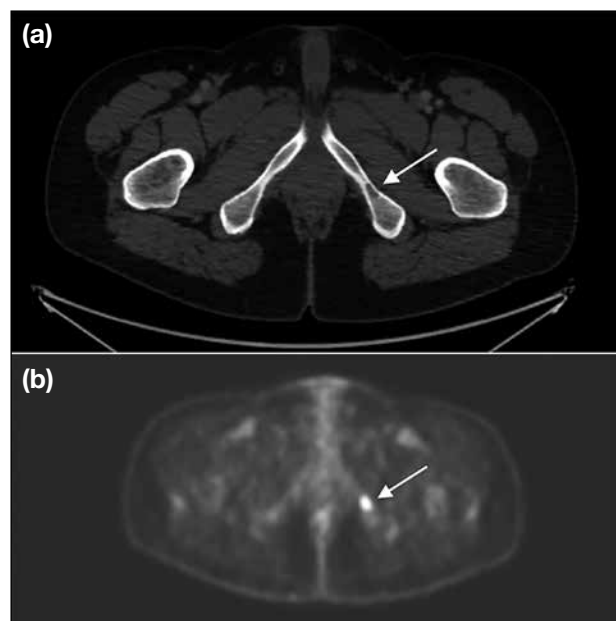


Figure 1. Positron emission tomography–computed tomography (PET-CT) demonstrating a lytic intramedullary lesion at the left ischiopubic ramus (arrows), with no periosteal reaction or soft tissue mass. The lesion exhibits hypermetabolic activity. (a) CT and (b) PET images.

Correspondence: Dr KH Chu, Department of Diagnostic and Interventional Radiology, Queen Elizabeth Hospital, Hong Kong SAR, China

Email: ckh975@ha.org.hk

Submitted: 24 October 2024; Accepted: 12 February 2025. This version may differ from the final version when published in an issue.

Contributors: KHC, WKK and LKT designed the study. KHC, WKK, LKT and JWL acquired the data. All authors analysed the data, drafted the manuscript, and critically revised the manuscript for important intellectual content. All authors had full access to the data, contributed to the study, approved the final version for publication, and take responsibility for its accuracy and integrity.

Conflicts of Interest: All authors have disclosed no conflicts of interest.

Funding/Support: This study received no specific grant from any funding agency in the public, commercial, or not-for-profit sectors.

Data Availability: All data generated or analysed during the present study are available from the corresponding author on reasonable request.

Ethics Approval: The study was approved by the Central Institutional Review Board of the Hospital Authority, Hong Kong (Ref No.: IRB-2024-502). Informed consent was obtained from the patient for the study and publication of this case report.

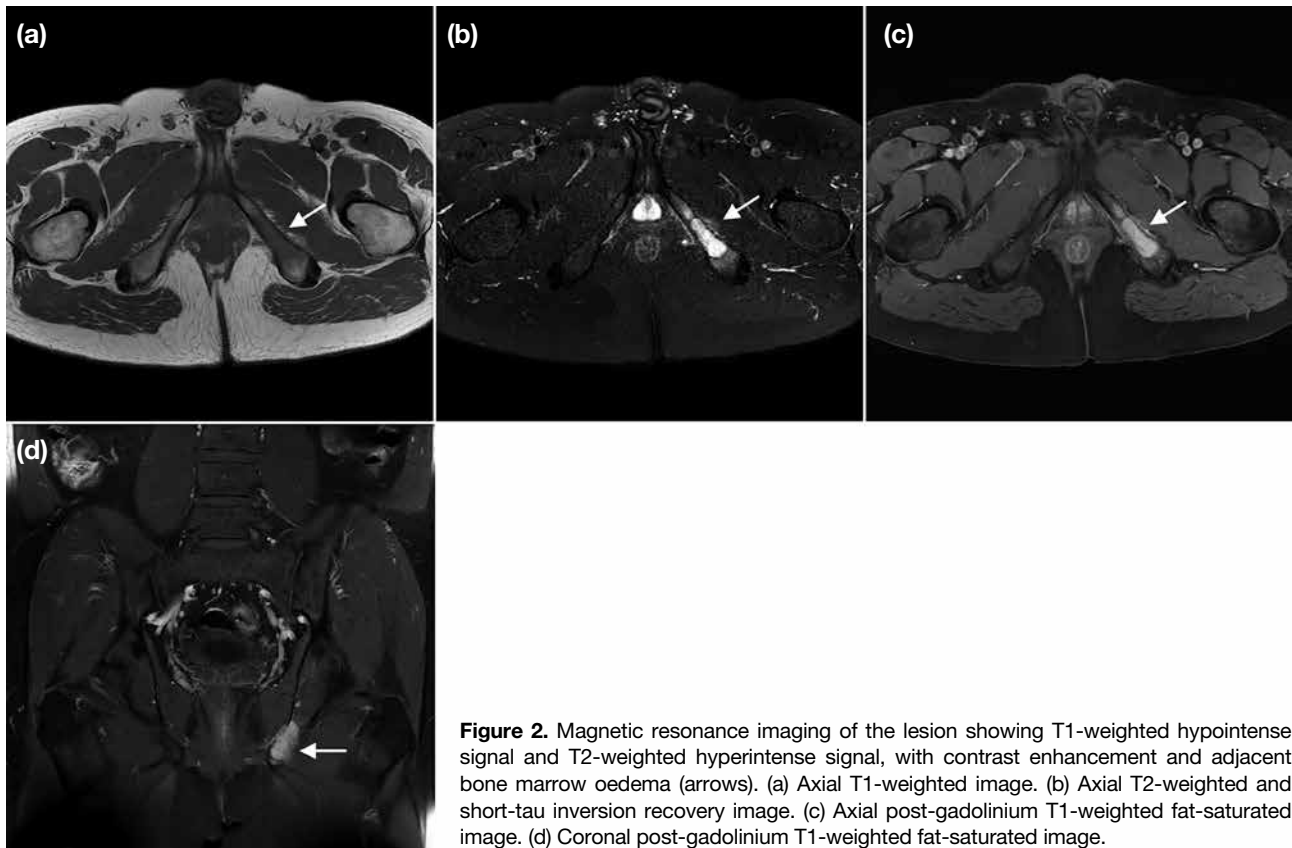


Figure 2. Magnetic resonance imaging of the lesion showing T1-weighted hypointense signal and T2-weighted hyperintense signal, with contrast enhancement and adjacent bone marrow oedema (arrows). (a) Axial T1-weighted image. (b) Axial T2-weighted and short-tau inversion recovery image. (c) Axial post-gadolinium T1-weighted fat-saturated image. (d) Coronal post-gadolinium T1-weighted fat-saturated image.

Results of the CT-guided biopsy of the lesion suggested a giant cell-rich spindle cell lesion, most compatible with an aneurysmal bone cyst. The biopsy showed random fascicles of spindle cells admixed with scattered osteoclast-type giant cells, accompanied by occasional lymphocytes, plasma cells and haemosiderin-laden macrophages. No atypical mitoses, marked nuclear pleomorphism, or necrosis were noted. Immunohistochemical study showed that the lesional cells were negative for H3G34W and H3K36M. Ubiquitin-specific protease 6 (*USP6*) gene translocation was identified by fluorescence in situ hybridisation.

Follow-up CT and MRI were performed prior to surgery, 2 months after the biopsy and 8 months after the initial imaging. The follow-up CT revealed interval enlargement of the lesion in the left ischiopubic ramus, with marked thinning of the medial cortex of the left ischium (Figure 3). Follow-up MRI demonstrated changes to the signal characteristics of the lesion, now

showing multiloculated cystic spaces with fluid-fluid levels and peripheral contrast enhancement along the wall and internal septa (Figure 4). There was no perilesional bone marrow oedema or extraosseous soft tissue extension.

Subsequently, the patient underwent curettage of the lesion, with allograft chips packed into the bone cavities. Pathological examination revealed tumour tissue featuring haphazardly arranged spindle cell fascicles and osteoclast-like multinucleated giant cells, set against a background of anastomosing woven bone trabeculae rimmed by osteoblasts and fibrous septa formed by bland fibroblasts (Figure 5). No cytological atypia, increased mitosis, or necrosis were observed. Immunohistochemical studies were once again performed, with the lesional cells being negative for H3G34W and H3K36M. The features were consistent with an aneurysmal bone cyst. To date, the patient has remained asymptomatic with no clinical evidence of tumour recurrence.



Figure 3. Follow-up computed tomography (CT) images showing interval enlargement of the lytic lesion (arrows) in the left ischiopubic ramus, with marked thinning of the medial cortex of the left ischium. (a) Axial CT image in bone window. (b) Coronal CT image in bone. (c) Coronal CT image in soft tissue window.

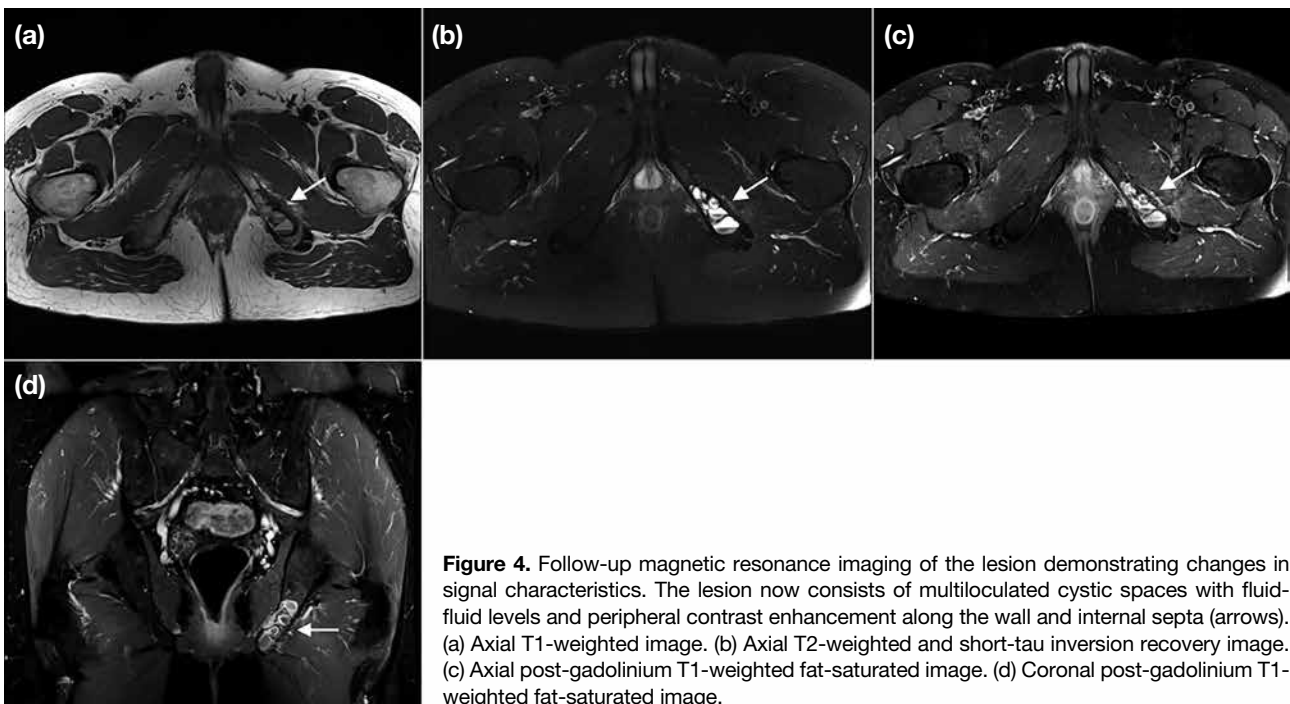


Figure 4. Follow-up magnetic resonance imaging of the lesion demonstrating changes in signal characteristics. The lesion now consists of multiloculated cystic spaces with fluid-fluid levels and peripheral contrast enhancement along the wall and internal septa (arrows). (a) Axial T1-weighted image. (b) Axial T2-weighted and short-tau inversion recovery image. (c) Axial post-gadolinium T1-weighted fat-saturated image. (d) Coronal post-gadolinium T1-weighted fat-saturated image.

DISCUSSION

Conventional aneurysmal bone cyst (ABC) refers to an expansile cystic lesion of bone composed primarily of blood-filled spaces. Although some solid areas may be present, these are not the predominant feature. Histologically, conventional ABC is characterised by blood-filled cystic spaces with septa containing fibroblasts, osteoclast-like giant cells, and reactive woven bone.¹ The solid variant of ABC is a rare entity that exhibits distinct radiological and pathological features. The cystic components may be completely absent, with the

lesion demonstrating a predominantly solid architecture. ABC was initially thought to represent a reactive and inflammatory response to intraosseous haemorrhage.² Nonetheless, with the identification of the *USP6* gene rearrangement, a translocation on chromosome 17p13, both conventional ABC and its solid variant are now considered true bone neoplasms.³ In the latest World Health Organization Classification of Tumors of Bone, ABC is classified as a benign osteoclastic giant cell-rich tumour.⁴ The term “aneurysmal bone cyst” is preferred over “primary aneurysmal bone cyst”, while “ABC-like

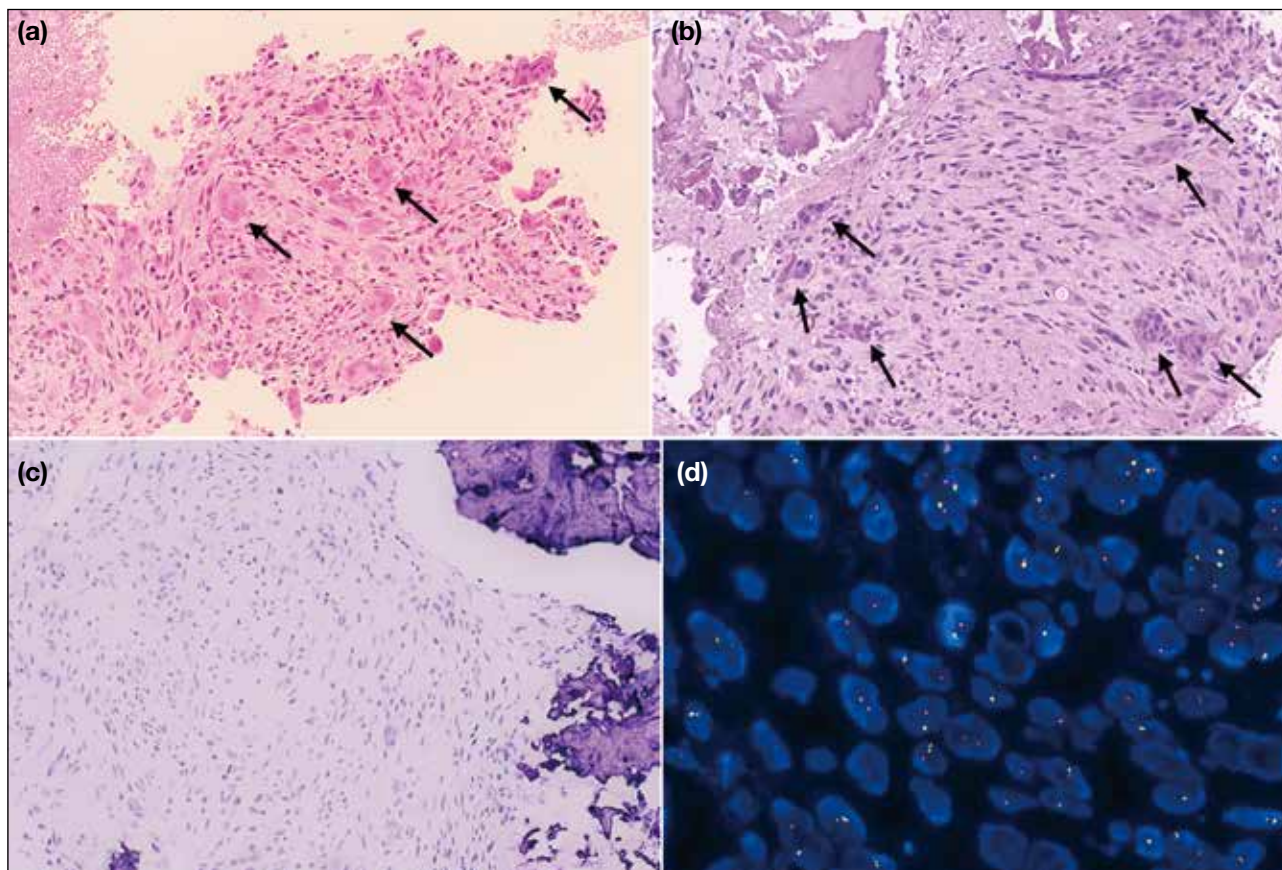


Figure 5. Computed tomography (CT)-guided biopsy and subsequent curettage reveal a giant cell-rich spindle cell lesion featuring fascicles of spindle cells admixed with scattered osteoclast-type giant cells (arrows in [a] and [b]), set against a background of anastomosing woven bone trabeculae. No atypical mitoses, marked nuclear pleomorphism, or necrosis are noted. The features are consistent with aneurysmal bone cyst. (a) CT-guided biopsy on haematoxylin and eosin stain (H&E) [× 40]. (b) Curettage specimen on H&E stain [× 100]. (c) Immunohistochemical study [× 100] showing negative staining for H3G34W in tumour cells. (d) Ubiquitin-specific protease 6 gene translocation detected by fluorescence in situ hybridisation break-apart probes.

change” is used instead of “secondary aneurysmal bone cyst”, the latter commonly observed in giant cell tumours of bone and chondroblastomas.

Reported cases of solid ABC (S-ABC) are primarily found in the metaphyseal and diaphyseal regions of long bones in children and young adults, typically during their second or third decade of life.⁵⁻⁸ These cases usually present with an insidious onset of pain, swelling, or a palpable mass. Although conventional ABC can involve the flat bones of the pelvis, S-ABC arising from pelvic bones in adults has not been reported, to the best of our knowledge. ABC in the pelvis is often asymptomatic due to its deep location, and by the time a patient develops symptoms, the lesion has typically reached a significant size. In our case, the lesion was an incidental finding

and relatively small without any complications; thus, the patient remains asymptomatic.

S-ABC can be confidently differentiated from conventional ABC on imaging. Although both can appear as lytic lesions with sclerotic margins on radiography and CT, conventional ABC typically exhibits an expansile soap bubble appearance with internal septa, whereas S-ABC often lacks septa and is non-expansile in up to one third of cases.⁵ Matrix mineralisation and periosteal reaction are generally absent in both forms.⁹ MRI is the modality of choice for aiding diagnosis. S-ABC is predominantly solid with uniform contrast enhancement, in contrast to the multiloculated cystic appearance and peripheral and septal enhancement seen in conventional ABC. Fluid-fluid levels can be observed in up to 70% of

conventional ABC cases but are not a consistent feature in S-ABC.⁷ Characteristically, S-ABC may be associated with mild bone marrow and soft tissue oedema in up to 50% of cases.⁸ The expansile nature of the lesion can lead to marked thinning and focal disruption of the bony cortex, as seen in our case during the initial presentation, mimicking an aggressive bony lesion. Interestingly, follow-up MRI after biopsy revealed multiple fluid-fluid levels, while the previously noted bone marrow and soft tissue oedema had resolved. Possible explanations for these changes include interval haemorrhage within the lesion due to the biopsy that could give rise to fluid-fluid levels. The bone marrow and soft tissue oedema may have resulted from an inflammatory response to the rapidly growing lesion in its initial phase, leading to cortical disruption.¹⁰

The diagnostic challenge of S-ABC lies in distinguishing it from ABC-like changes and other solid bone tumours. The main differential diagnoses include giant cell tumour of bone (GCTB), chondroblastoma, and primary bone malignancies such as telangiectatic osteosarcoma. GCTB typically occurs in a slightly older patient population, demonstrates non-sclerotic margins, and often extends to the subarticular surface of long bones. Immunohistochemical staining for H3G34W and H3K36M are specific markers that aid differentiation; they are present in GCTB and chondroblastoma with or without ABC-like changes, but are absent in ABC.¹¹ In contrast, telangiectatic osteosarcoma is characterised by geographic bone destruction, wide zones of transition, and dense osteoid mineralisation. Extensive soft tissue involvement and cortical destruction, along with periosteal reaction on MRI, raise suspicion for a malignant tumour rather than S-ABC.¹²

Biopsy and pathological examination are often necessary when evaluating an aggressive-appearing lesion, and radiological-pathological correlation plays a pivotal role in reaching a diagnosis. S-ABC is characterised by fibroblastic proliferation, osteoclast-like giant cells, and focal osteoid production. In contrast to conventional ABC, the blood-filled cystic spaces are present only in small amounts, if at all. Histologically, S-ABC resembles giant cell reparative granuloma and brown tumours of hyperparathyroidism, as all three entities exhibit giant cells, haemorrhagic areas, and reactive osteoid formation.⁸ Nonetheless, they lack the *USP6* gene rearrangement.¹³ Historically, the term S-ABC was used interchangeably with giant cell reparative

granuloma; however, they are now regarded as distinct entities, with the latter term reserved for lesions in the gnathic location.¹⁴ It is important to note that *USP6* gene rearrangement is not exclusive to ABCs; it has also been identified in several other lesions, including nodular fasciitis, myositis ossificans, fibro-osseous pseudotumour of the digits, and cellular fibroma of the tendon sheath. The diagnosis of S-ABC can be established through a combination of compatible radiological features and pathological examination.

CONCLUSION

S-ABC presents a unique diagnostic challenge due to its similarities to other aggressive bone lesions. Accurate diagnosis requires a comprehensive approach that includes imaging, histological evaluation, and identification of the *USP6* gene rearrangement. Radiologists should be aware of the distinct features of S-ABC, particularly in contrast to conventional ABC and other lesions such as giant cell tumour and telangiectatic osteosarcoma.

REFERENCES

1. Nasri E, Reith JD. Aneurysmal bone cyst: a review. *J Pathol Transl Med*. 2023;57:81-7.
2. Sato K, Sugiura H, Yamamura S, Takahashi M, Nagasaka T, Fukatsu T. Solid variant of an aneurysmal bone cyst (giant cell reparative granuloma) of the 3rd lumbar vertebra. *Nagoya J Med Sci*. 1996;59:159-65.
3. Cordier F, Creytens D. Unravelling the *USP6* gene: an update. *J Clin Pathol*. 2023;76:573-7.
4. Choi JH, Ro JY. The 2020 WHO Classification of Tumors of Bone: an updated review. *Adv Anat Pathol*. 2021;28:119-38.
5. Ghosh A, Singh A, Yadav R, Khan SA, Kumar VS, Gamanagatti S. Solid variant ABC of long tubular bones: a diagnostic conundrum for the radiologist. *Indian J Radiol Imaging*. 2019;29:271-6.
6. Restrepo R, Zahrah D, Pelaez L, Temple HT, Murakami JW. Update on aneurysmal bone cyst: pathophysiology, histology, imaging and treatment. *Pediatr Radiol*. 2022;52:1601-14.
7. Al-Shamy G, Relyea K, Adesina A, Whitehead WE, Curry DJ, Luerssen TG, et al. Solid variant of aneurysmal bone cyst of the thoracic spine: a case report. *J Med Case Rep*. 2011;5:261.
8. Ilaslan H, Sundaram M, Unni KK. Solid variant of aneurysmal bone cysts in long tubular bones: giant cell reparative granuloma. *AJR Am J Roentgenol*. 2003;180:1681-7.
9. Yamaguchi T, Dorfman HD. Giant cell reparative granuloma: a comparative clinicopathologic study of lesions in gnathic and extragnathic sites. *Int J Surg Pathol*. 2001;9:189-200.
10. Mahnken AH, Nolte-Ernsting CC, Wildberger JE, Heussen N, Adam G, Wirtz DC, et al. Aneurysmal bone cyst: value of MR imaging and conventional radiography. *Eur Radiol*. 2003;13:1118-24.
11. Schaefer IM, Fletcher JA, Nielsen GP, Shih AR, Ferrone ML, Hornick JL, et al. Immunohistochemistry for histone H3G34W and H3K36M is highly specific for giant cell tumor of bone and chondroblastoma, respectively, in FNA and core needle biopsy. *Cancer Cytopathol*. 2018;126:552-66.

12. Zishan US, Pressney I, Khoo M, Saifuddin A. The differentiation between aneurysmal bone cyst and telangiectatic osteosarcoma: a clinical, radiographic and MRI study. *Skeletal Radiol.* 2020;49:1375-86.
13. Oliveira AM, Perez-Atayde AR, Inwards CY, Medeiros F, Derr V, Hsi BL, et al. *USP6* and *CDH11* oncogenes identify the neoplastic cell in primary aneurysmal bone cysts and are absent in so-called secondary aneurysmal bone cysts. *Am J Pathol.* 2004;165:1773-80.
14. Lee JC, Huang HY. Soft tissue special issue: giant cell-rich lesions of the head and neck region. *Head Neck Pathol.* 2020;14:97-108.